Loss of endothelial miR-126 drives age-related decline in hematopoiesis

Dandan Zhao,[1*] Le Xuan Truong Nguyen,[1*] Xubo Gong,[1,2*] Fang Chen,[1] Xiaoli Zhao,[1] Min-Hsuan Chen,[3] Guido Marcucci[1] and Bin Zhang[1]

[1]Department of Hematological Malignancies Translational Science, Gehr Family Center for Leukemia Research, City of Hope National Medical Center and Beckman Research Institute, Duarte, CA, USA; [2]Department of Clinical Laboratory, The Second Affiliated Hospital, Zhejiang University School of Medicine, Hangzhou, Zhejiang, P.R. China and [3]Integrative Genomics Core, Department of Computational and Quantitative Medicine, City of Hope Beckman Research Institute, Duarte, CA, USA

**DZ, LXTN and XG contributed equally as first authors.*

Correspondence: B. Zhang
bzhang@coh.org

G. Marcucci
gmarcucci@coh.org

Received: July 17, 2025.
Accepted: November 25, 2025.
Early view: December 4, 2025.

https://doi.org/10.3324/haematol.2025.288736

Abstract

Aging profoundly alters the bone marrow (BM) microenvironment and impairs hematopoietic stem cell (HSC) function. Here, we identify decrease of miR-126 derived from arteriolar endothelial cells (EC) as a key mechanism of impaired HSC self-renewal capacity during aging. In young BM, arteriolar EC express high levels of miR-126, which is transferred to HSC and supports these cells' homeostasis and functional integrity. Using young and aged wild-type, endothelial-specific miR-126 knockout (EC-miR-126 KO), EC-Spred1 knockout (a functional model of EC-miR-126 upregulation), and EC/Sca-1 dual fluorescent reporter mice, we show that age-related increase in inflammatory cytokines (such as TNFα) reduces EC miR-126 expression and in turn drives loss of miR-126^{high} CD31^{+}Sca-1^{high} EC-lined arterioles in the aging BM niche. Loss of arterioles in turn decreases the EC miR-126 supply to HSC, leading to expansion of HSC with limited self-renewal capacity. Remarkably, administration of a synthetic miR-126 mimic oligonucleotide restores EC-HSC communication and rescues aging-related HSC dysfunction. Our findings uncover a novel, non-cell-autonomous mechanism of HSC aging and highlight EC-derived miR-126 as a promising therapeutic target to rejuvenate hematopoiesis.

Introduction

Adult hematopoiesis is sustained by hematopoietic stem cells (HSC) residing in the bone marrow (BM). These primitive cells possess the capacity for self-renewal, expansion, and differentiation.[1,2] Although HSC appear morphologically and immunophenotypically similar, there is growing evidence to indicate that they are functionally heterogeneous, comprising distinct subsets with lineage-biased transcriptomic profiles.[1,3-5] These subsets eventually give rise to lineage-committed progenitor cells, which further differentiate into mature blood and immune cells.[1,3-5]

The aging hematopoietic system presents with increased myelopoiesis, impaired adaptive immunity, and a functional decline of the HSC, despite their increased frequency as compared with young counterparts.[1,4-9] The HSC functional decline is characterized by reduced regenerative potential, impaired homing ability, loss of cell polarity, and a shift toward myeloid-biased differentiation at the expense of lymphopoiesis.[6,7,10] The mechanisms underlying these age-related changes are not yet fully understood but likely involve several mechanisms including DNA damage,[11,12] mitochondrial dysfunction,[13,14] inflammation,[15,16] and dysregulation of replication stress responses,[17,18] DNA repair pathways,[19,20] and metabolic processes,[21,22] among others.[10]

Hematopoietic stem cells reside within a specialized BM microenvironment known as the "HSC niche", which is composed of various stromal cell types including endothelial cells (EC), mesenchymal stromal cells (MSC), osteoblasts, and extracellular matrix components; altogether the niche regulates HSC function and homeostasis.[23-25] Functional deterioration of HSC during aging may arise from alterations of intrinsic cellular processes,[6] including a metabolic shift from glycolysis in young HSC to oxidative metabolism in aged HSC,[10] as well as from changes extrinsic to HSC and characterizing other components of the BM niche.[23,24] Altogether, these changes can lead to a decline in HSC function, including reduced self-renewal, impaired differentiation, and increased susceptibility to malignant transformation.[23,24] Notably, aged HSC transplanted into young recipients exhibit reduced myeloid output compared to those transplanted into aged recipients, implicating the

aged BM microenvironment in the skewing of hematopoiesis toward the myeloid lineage.[26]

The BM niche is highly vascularized, and HSC are primarily localized in perivascular regions.[27] Different classifications of BM vessels have been reported based on the staining of distinct markers. These include: CD31^{+}Sca-1^{high}endomucin (Emcn)$^{-}$ arterioles, CD31^{+}Sca-1^{low}Emcn^{low} sinusoids, and CD31^{+}Emcn^{high} type H vessels, a type of capillary found in the metaphysis and endosteum of long bones and connecting arterioles to sinusoids.[27-31] Prior studies have highlighted a critical interplay between BM vasculature and hematopoiesis, with arterioles playing a protective and supportive role for HSC.[27,31] *Ex vivo* co-culture of aged EC with young HSC, as well as *in vivo* infusion of aged EC in mice following myelosuppression, suggested that aged EC impaired the repopulating activity of young HSC and contributed to myeloid bias of aged HSC; conversely, infusion of young EC restored the balanced repopulating capacity of aged HSC,[32] indicating an active interplay between the vascular component of the BM niche and HSC during aging. However, the molecular mechanisms of this interaction and the resulting phenotypic changes are still not completely understood.

MicroRNA (miRNA) are short non-coding RNA that regulate gene expression post-transcriptionally. MiRNA reportedly play a role in regulating various hallmarks of aging, such as DNA damage response, cellular senescence, and mitochondrial dysfunction.[33] Genome-wide miRNA profiling of blood samples from long-lived individuals (mean age 96.4 years) and younger controls (mean age 45.9 years) showed a decrease of miR-126 levels with age.[34] miR-126 reportedly regulates glucose and lipid metabolism in cancer and adipose cells via inhibiting IRS1/Akt axis.[35-37] Of note, while miR-126 is highly expressed in arteriolar CD31^{+}Sca-1^{high} EC and acts as a master regulator of physiological angiogenesis,[38-40] it also plays a pivotal role in regulating HSC self-renewal.[40-44] We previously reported that arteriolar EC supply miR-126 to the BM niche and that disruption of miR-126 biogenesis leads to a reduction in CD31^{+}Sca-1^{high} EC-lined arterioles, accompanied by a subsequent decline in EC miR-126 supply to normal or clonal HSC.[43,45] Understanding how the interplay between HSC and the vascular component of the BM niche is disrupted during aging is crucial for developing strategies to rejuvenate the HSC function in older individuals.

In this study, we identified changes in EC miR-126 production as a key factor in inducing age-related HSC dysfunction. We showed that aging is associated with increased levels of pro-inflammatory cytokines such as TNFα, which leads to downregulation of EC miR-126, loss of arterioles, and in turn decreased EC miR-126 supply to HSC. Consequently, HSC expand, but at the expense of their self-renewal capacity. Thus, supplementing synthetic miR-126 mimic to the aging BM niche rescued the age-related hematopoietic changes.

Methods

Mouse strains

Unless otherwise indicated, 2-3-months old and 18-24-months old C57Bl/6J (B6, CD45.2) mice were respectively categorized as young and aged mice. *Tie2-CreER/TdTomato/Tg(Ly6a-GFP)* double fluorescent reporter mice[45] were used to visualize CD31^{+}Sca 1^{high} (tdTomato^{+}GFP^{high}) and CD31^{+}Sca-1^{low} (tdTomato^{+}GFP^{low}) EC-lined vessels. *Mir126*$^{floxf/f}$ *fTie2-cre+* (i.e., EC-miR-126 knock-out [KO]) and *Spred1*$^{f/f}$ *Tie2-cre+* (EC-Spred1 KO, representing a functional model of EC-miR-126 overexpression [OE]) mice[45,46] were used to obtain miR-126 KO or OE in EC. To obtain conditional EC-miR-126 KO reporter mice, we also bred *Tie2-CreER/TdTomato* reporter mice with *Mir126*$^{f/f}$ mice and obtained inducible EC-miR-126 KO reporter mice (i.e., *Mir126*$^{f/f}$*/Tie2-CreER/TdTomato*, miR-126 KO in EC upon tamoxifen administration). Mouse care and experimental procedures were performed in accordance with federal guidelines and protocols. Procedures were approved by the Institutional Animal Care and Use Committee at the City of Hope under protocol IACUC 15005.

Immunofluorescent staining and 3D confocal imaging of long bones

Long bones (tibias) from the mice were processed, sectioned, and imaged, as described previously.[45-47]

Intravital imaging

Intravital confocal microscopy was used to image the calvarium BM vasculature to study the vascular permeability, as previously described.[45,48]

Flow cytometry analysis

Mouse cells were obtained from peripheral blood (PB) or BM (from both tibias and femurs). Before staining for HSC, c-Kit^{+} cells were selected using anti-mouse CD117 microbeads or Lineage^{-} (Lin^{-}) cells were selected using mouse Lineage cell depletion kit (both from Miltenyi Biotec, San Diego, CA, USA). EC were isolated from long bones (tibias and femurs) of the mice, as previously described.[45] Cells were stained with anti-mouse antibodies (*Online Supplementary Table S1*). HSC were identified as Lin^{-}Sca-1^{+}c-Kit^{+} (LSK) Fit3^{-}CD150^{+}CD48^{-}. EC were identified as CD45^{-}Ter119^{-} CD31^{+}. All analyses were performed on a Fortessa x20 flow cytometer (BD Biosciences) and sorting was performed on Aria Fusion instrument (BD Biosciences); data were analyzed by BD FACSDiva or FlowJo software.

RNA sequencing

Total RNA was extracted from BM HSC (Fit3^{-}CD150^{+}CD48^{-} LSK) sorted from young (2-3-months old) and aged (18-24-months old) mice using the miRNeasy micro Kit (Qiagen, Valencia, CA, USA). Sequencing was performed on an Illumina NovaSeq 6000 platform using the S4 Reagent

Kit v1.5 in paired-end mode (2x101 cycles). The HTSeq software (v.0.11.1)[49] was applied to generate the count matrix, with default parameters. Differentially expressed gene (DEG) analysis was conducted by adjusting read counts to normalized expression values using TMM normalization method in edgeR.[50,51] Genes with an FDR-adjusted *P* value <0.05 and with a fold change (FC) >2 or <0.5 were considered as significantly up- and down-regulated genes, respectively. Pathway analysis was conducted using Gene Set Enrichment Analysis (GSEA) algorithm implemented in clusterProfiler (v.4.14.3) package in R,[52-55] where a ranked list of whole genes according to their log2 fold change and *P* values are provided.

Statistical analysis

All statistical analyses were performed using Prism version 10.0 software (GraphPad). Sample sizes chosen are indicated in the individual figure legends. All *in vitro* experiments were performed 2-3 times using biologically independent samples; *in vivo* experiments were performed using 6-15 mice in each group. Results were reported as mean ± standard error of the mean or standard deviation. Comparisons between groups were performed by a two-tailed, unpaired Student *t* test.

Further details of the methods used are available in the *Online Supplementary Appendix*.

Results

Self-renewal and repopulating capacities of aged hematopoietic stem cells

To prioritize the relative contributions of intrinsic *versus* extrinsic factors that impact on self-renewal and repopulating capacities of aging HSC, we transplanted BM HSC (Fit3$^-$CD150$^+$CD48$^-$ LSK) from young (2-3-months old) and aged (18-24-months old) CD45.2 C57BL/6j wild-type (wt) mice into age-matched young (N=10 recipient mice for young HSC donor; N=9 recipient mice for aged HSC donor) and aged (N=7 recipient mice for young HSC donor; N=6 recipient mice for aged HSC donor) CD45.1 C57BL/6j wt recipient mice (200 cells/mouse) (Figure 1A). Transplanted HSC from aged mice had consistently exhibited reduced self-renewal and reconstitution capacities compared with transplanted HSC from young mice, regardless of the recipient age (aged *vs*. young HSC engraftment at 24 weeks post transplant: 5.5% *vs*. 41.3%, *P*<0.0001 in young recipients; 1.167% *vs*. 25.93%, *P*=0.001 in aged recipients) (Figure 1B, top two panels). We also observed that the donor HSC long-term engraftment rates were consistently lower in the aged recipients compared with the young recipients, regardless of donor age (engraftment at 24 weeks post transplant in aged *vs*. young recipients: 25.9% *vs*. 45.2% for young donor HSC, *P*=0.0034; 1.17% *vs*. 5.53% for aged donor HSC, *P*=0.01) (Figure 1B, bottom two panels).

We observed an approximately 10-fold enrichment of BM HSC in aged mice compared with young mice (Figure 1C), and a reduced regenerating capacity of aged HSC compared to the younger counterparts, indicating that the diminished function is partly counterbalanced by increased numbers to maintain HSC function. To factor in the approximately 10-fold enrichment of BM HSC found in aged *versus* young mice (Figure 1C), and reflect the overall regenerating capacity of the increased HSC in aged *versus* young mice, we transplanted both young and aged recipients with young or aged HSC collected from the same numbers of young or aged mice. Briefly, we pooled HSC (Fit3$^-$CD150$^+$CD48$^-$ LSK) from 5 young (2-3-months old) or 5 aged (18-24-months old) CD45.2 C57BL/6j wt mice, yielding a total of 6,021 young and 61,157 aged HSC, respectively, and transplanted them into 15 young and 15 aged CD45.1 C57BL/6j wt recipient mice (approximately 200 young HSC or 2,000 aged HSC per mouse; N=15 mice per group) (*Online Supplementary Figure S1A*) that were monitored for engraftment rates every four weeks. We observed that regardless of recipient age, aged HSC (2,000/mouse) showed the highest engraftment rates at four weeks post transplant followed by a progressive decline in hematopoiesis over time, while young HSC (200/mouse) showed the lowest engraftment rates at four weeks followed by a robust increase over time (*Online Supplementary Figure S1B*, top two panels). Thus, regardless of the age and number of the received HSC, long-term PB and BM engraftment rates were always lower in the aged recipients than in the young recipients (PB engraftment at 16 weeks: 19.7% *vs*. 38.5% for young HSC, *P*=0.0007; 14.8% *vs*. 26.0% for aged HSC, *P*=0.002) (*Online Supplementary Figure S1B*, bottom two panels, and *Online Supplementary Figure S1C*). These results highlight that hematopoiesis and regenerative capacity do not depend only on the age of HSC but also on that of the BM microenvironment.

Vascular remodeling in the aged bone marrow niche

The vascular compartment of the BM niche has been shown to affect HSC functionality.[27] To determine age-related changes in the vascular compartment of the BM niche, we performed immunofluorescence staining and 3D confocal imaging of vessels in tibias from 2-, 10- and 20-months old wt mice, representing young, middle-aged, and aged groups. Sca-1^{high} EC line arteries and arterioles while Sca-1^{low} EC line sinusoids;[45] type H vessels are characterized by high expression of CD31 and Emcn, and are located in the metaphysis and endosteum of long bones.[56] Here, we utilized a simplified CD31$^+$Sca-1^{high}, CD31$^+$Sca-1^{low} and CD31$^+$Emcn^{high} staining combined with morphology examination and anatomical location to identify BM arterioles, sinusoids and type H vessels, respectively (*Online Supplementary Figure S2A*), as reported by us and others.[45,46,56] Consistent with the previous finding that type H vessels are reduced in aged mice,[56] we also observed a depletion of CD31$^+$Emcn^{high} type H vessels in metaphysis of the long

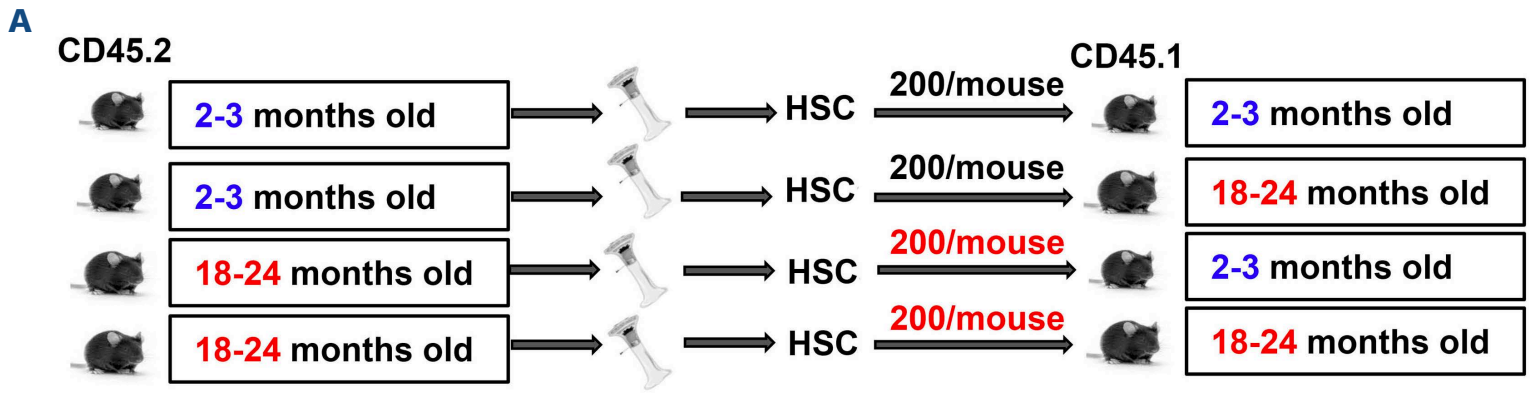

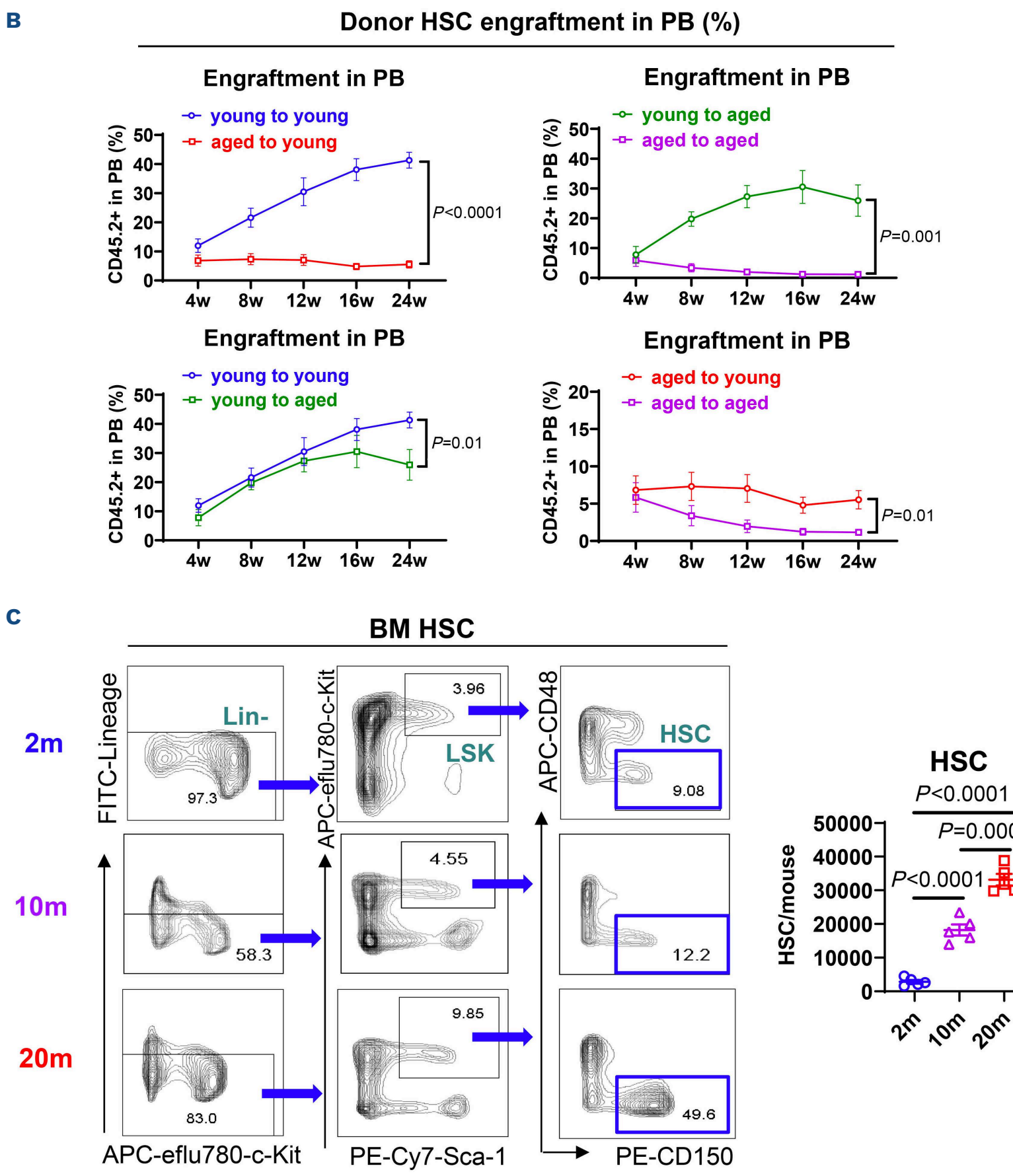

Figure 1. Aged bone marrow niche impacts long-term regenerating capacity of hematopoietic stem cells. (A and B) Schematic experimental design and results. Lineage$^-$Sca-1$^+$c-Kit$^+$FLT3$^-$CD150$^+$CD48$^-$ hematopoietic stem cells (HSC, 200/mouse) from young (2-3 months old) and aged (18-24 months old) C57BL/6j mice (B6, CD45.2) were sorted and transplanted into age-matched young (young HSC: N=10; aged HSC: N=9) and aged (young HSC: N=7; aged HSC: N=6) recipients (CD45.1), respectively (A). Then donor HSC engraftment rates in peripheral blood (PB) of aged recipients *versus* young recipients were monitored every four weeks (w) by flow cytometry

analysis (B). (C) Representative plots (left) and combined results (right) showing Lineage$^-$Sca-1$^+$c-Kit$^+$FLT3$^-$CD150$^+$CD48$^-$ HSC in the bone marrow (BM) of 2, 10 and 20 months (m) old mice analyzed by flow cytometry. Statistical analysis was calculated by two-tailed, unpaired Student *t* test. Results shown represent mean ± standard error of mean.

bone from aged *versus* young mice (*Online Supplementary Figure S2B*), which was confirmed by flow cytometry (*Online Supplementary Figure S2C*). Of note, flow cytometry analysis of metaphysis region of femurs showed that almost all Emcn^{high} EC are Sca-1^{high} in both young and aged mice (*Online Supplementary Figure S2C*, left). Notably, we detected a significant decrease in CD31$^+$Sca-1^{high} EC-lined arterioles in metaphysis and diaphysis of long bones in the aged mice compared with the young mice (Figure 2A, B and *Online Supplementary Figure S3*). These results were corroborated by flow cytometry analysis showing an overall decrease in total BM EC (CD45$^-$Ter119$^-$CD31$^+$) in the aged mice, with a significantly lower frequency of CD31$^+$Sca-1^{high} EC that line mainly arterioles, and a higher frequency of CD31$^+$Sca-1^{low} EC that line sinusoids, compared with the young mice (Figure 2C-E). Similar results were also obtained in a genetically modified model carrying tamoxifen-induced Tie2-CreER/TdTomato/Tg(Ly6a-GFP) double-fluorescent reporter that allowed us to track EC (EC-TdTomato$^+$, Sca-1-GFP^{high}).[45] We observed reduced BM CD31-tdTomato$^+$Sca-1-GFP^{high} EC-lined arterioles in the aged double reporter mice compared with the young double reporter mice (Figure 3A, B). Consistent with these results, flow cytometry analysis showed reduced Sca-1^{high} EC (i.e., tdTomato$^+$ GFP^{high}) and increased Sca-1^{low} EC (i.e., tdTomato$^+$ GFP^{low}) in the aged *versus* young reporter mice (Figure 3C-E).

In the BM niche, CD31$^+$Sca-1^{high} EC reportedly line impermeable vessels such as arterioles, and CD31$^+$Sca-1^{low} EC border permeable vessels such as sinusoids.[45,57] Thus, we imaged the mouse calvaria with intravital confocal microscopy. Prior to imaging, mice were administered with FITC-dextran (150 kDa, green) intravenously to label the vasculature.[45] Consistent with a decrease in CD31$^+$Sca-1^{high} arterioles in the aged mice (Figure 2A, B), we also observed increased vessel permeability, as evidenced by the leakage of FITC-dextran as diffuse staining in the calvarium by intravital confocal microscopy (FITC-150 kDa dextran, green) compared with the young mice (*Online Supplementary Figure S4A, B*).

Taken together, these findings are consistent with age-associated loss of arterioles and compensatory enrichment of fenestrated sinusoids in the bone marrow.

"Inflammaging" induces bone marrow endothelial cell miR-126 downregulation

Chronic inflammation in the aging BM niche, also known as "inflammaging",[16,58] impacts HSC function.[59-61] We previously reported that in pathologic conditions (i.e., acute myeloid leukemia), blast-derived cytokines (i.e., TNFα) suppresses miR-126 production, leading to a loss of arterioles.[45] We, therefore, hypothesized that inflammaging may also lead to downregulation of EC miR-126, loss of arterioles, and reduced EC-derived miR-126 supply to HSC. To test this hypothesis, we first showed that levels of pro-inflammatory cytokines are generally higher in aged (18-24-months old C57BL/6j, N=14) mice compared with gender-matched young (2-3-months old, N=10) mice (*Online Supplementary Figure S5*). Next, we treated mouse EC with a panel of cytokines (including TNFα, IFNγ, IL-1α, IL-4, IL-10, IL-13, IL-16, M-CSF, MCP-5, MIP-1α, MIP-2, RANTES, CXCL12, TNFSF12, TNFSF13B, TNFSF6 and angiopoietin-2) at two concentrations, one as measured in young BM plasma and one as in aged BM plasma by Luminex assay, for eight hours, and observed the lowest levels of miR-126 in EC treated with TNFα at the concentration measured in aged BM plasma (Figure 4A). In the aged mice, we also observed a BM expansion of the myeloid cells expressing significantly higher levels of TNFα (*Online Supplementary Figure S6A, B*). This was associated with a significant reduction in primary (pri), precursor (pre), and mature miR-126 levels in BM EC (Figure 4B) and loss of BM CD31$^+$Sca-1^{high} EC and arterioles (Figure 2A-E) in the aged mice compared with the young mice. We confirmed these results in the aged double reporter mice (i.e., tamoxifen-induced Tie2-CreER/TdTomato/Tg[Ly6a-GFP]) that have a significant reduction in EC-miR-126 expression (*Online Supplementary Figure S6C*) and loss of BM CD31-tdTomato$^+$Sca-1-GFP^{high} EC-lined arterioles (Figure 3A, B) compared with the young reporter mice. Treatment of BM EC from young mice with murine recombinant (mr) TNFα (1 ng/mL, 8 hours) resulted in reduction in EC pri-, pre- and mature miR-126 levels and Sca-1^{high} subset (*Online Supplementary Figure S6D*); these changes were largely rescued by co-treatment with TNFαR1/R2 blocking antibodies (1 μg/mL) (*Online Supplementary Figure S6E*). Importantly, treatment of young wt mice with mrTNFα (interperitoneal [i.p.] 1 μg/day, 3 weeks) (Figure 4C) recapitulated the findings we observed in the aged mice, i.e., decreased BM EC pri-, pre-, and mature miR-126 levels (Figure 4D) and a reduction of arteriole-lining CD31$^+$Sca-1^{high} EC (Figure 4E, middle panel). Notably, co-treatment with a synthetic miR-126 mimic oligonucleotide (M-miR-126)[43,45] rescued TNFα-induced loss of CD31$^+$Sca-1^{high} EC (Figure 4E, right panel). To determine how TNFα induces endothelial miR-126 downregulation, we measured levels of transcription factors Ets1, Ets2 and Gata2 that are verified regulators of miR-126 expression.[62,63] We observed significant reduction of Gata2, and not of Ets1 and Ets2, in EC treated with mrTNFα (*Online Supplementary Figure S7A*). We also demonstrated reduced Gata2 levels in aged BM EC *versus* young BM EC (*Online Supplementary Figure S7B*) and that GATA2 knockdown (KD) by siRNA in young BM EC decreased miR-126 levels (*Online Supplementary Figure S7C*). Using chromatin immunoprecipitation assay, we showed a reduced GATA2 enrichment on the

EGFL7/miR-126 promoter[64] in EC exposed to TNFα (1 ng/mL) (*Online Supplementary Figure S7D*). Collectively, these results support the hypothesis that loss of CD31⁺Sca-1^{high} EC and associated vessels (i.e., arterioles) during aging is at least partly mediated by EC miR-126 downregulation via TNFα-induced decrease of GATA2 transcriptional activity. The vascular changes seen in the aged BM niche were strikingly similar to what we observed in the young *Mir-*

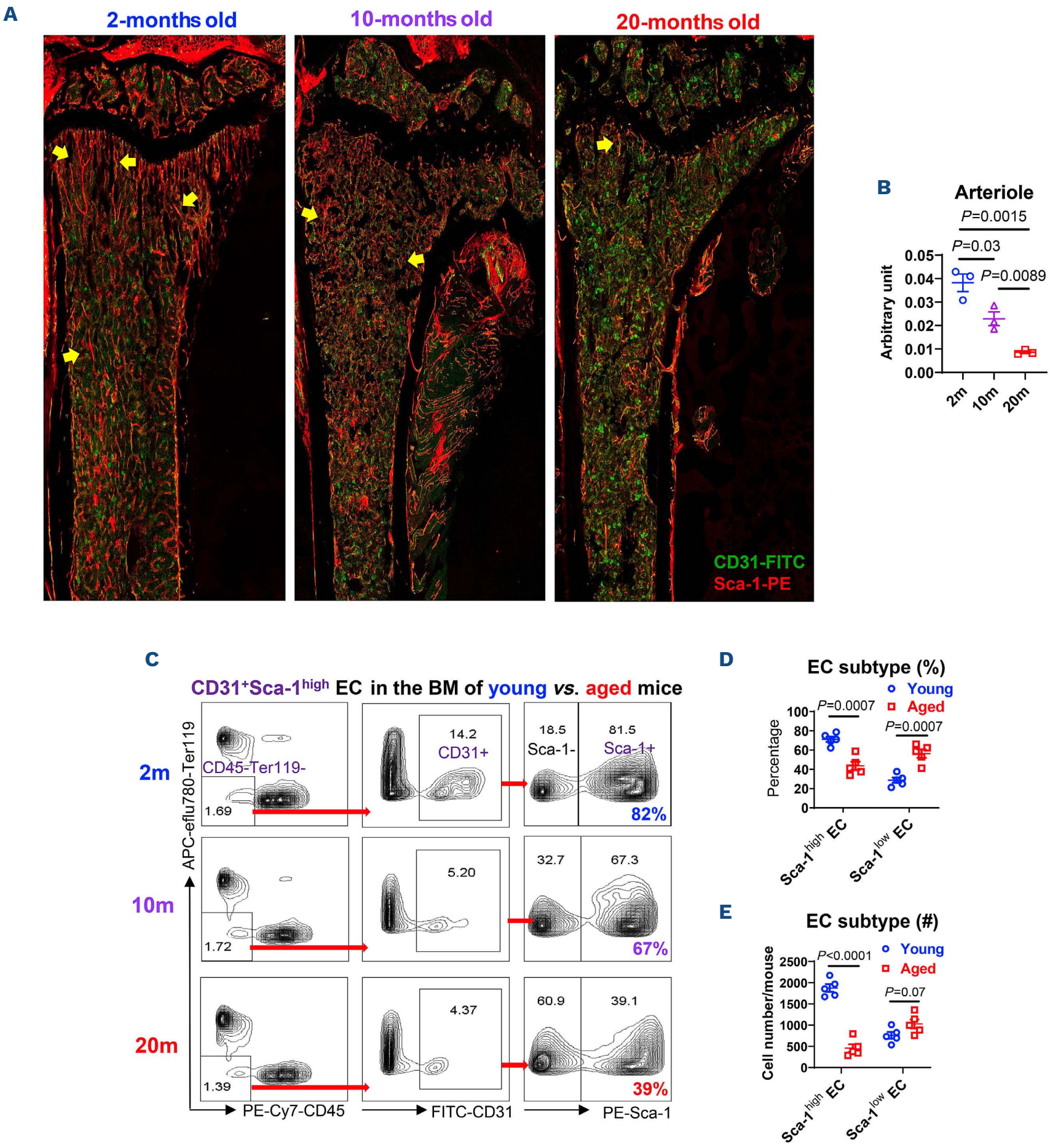

Figure 2. Vascular remodeling of the aged bone marrow niche. (A and B) CD31 (FITC) and Sca-1 (PE) immunofluorescence staining (A) and quantification (B) of CD31⁺Sca-1^{high} endothelial cell (EC)-lined arterioles in tibias from 2-, 10-, and 20-months old mice, assessed by immunofluorescent staining and 3D confocal imaging. (A) One of the three independent experiments with similar results is shown; yellow arrows indicate CD31⁺Sca-1^{high} EC-lined arteriolar vessels. (C-E) Representative plots (C) and combined results showing frequencies (D) and absolute counts (E) of Sca-1^{high} and Sca-1^{low} EC subfractions in bone marrow (BM) CD45⁻Ter119⁻CD31⁺ EC from 2-, 10-, and 20-months (m) old mice, analyzed by flow cytometry. Statistical analysis was calculated by two-tailed, unpaired Student *t* test. Results shown represent mean ± standard error of mean.

126$^{flox(f)/f}$*Tie2-cre*$^{+}$ mice (a model of EC-miR-126 KO) (*Online Supplementary Figure S8A*), which also had fewer CD31^{+}Sca-1^{high} EC and arterioles than young wt controls (*Mir126*$^{f/f}$*Tie2-cre*$^{-}$ mice) (Figure 5A-D); these changes were even more pronounced in the aged *Mir126*$^{f/f}$*Tie2-cre*$^{+}$ mice (*Online Supplementary Figure S8A-E*). To this end, we also observed increased vessel permeability, as evidenced by the leakage of FITC-dextran in the calvarium by intravital confocal microscopy, in the young EC-miR-126 KO reporter mice (i.e., tamoxifen-induced *Mir126*$^{f/f}$*/Tie2-CreER+/TdTomato*, CD31-TdTomato^{+} and EC-miR-126 KO), compared with the young wt reporter mice (i.e., tamoxifen-induced Tie2-CreER+/TdTomato, CD31-TdTomato+; FITC-150 kDa dextran, green) (*Online Supplementary Figure S9A-C*), supporting the vascular changes. Conversely, we did not observe these changes in EC-miR-126 OE mice. We previously reported that Spred1, a member of the Sprouty family of proteins and an inhibitor of RAS small GTPases, is both an miR-126 target, as confirmed here by repressed activity of Spred1 3' UTR luciferase reporter in mouse EC by M-miR-126 (*Online*

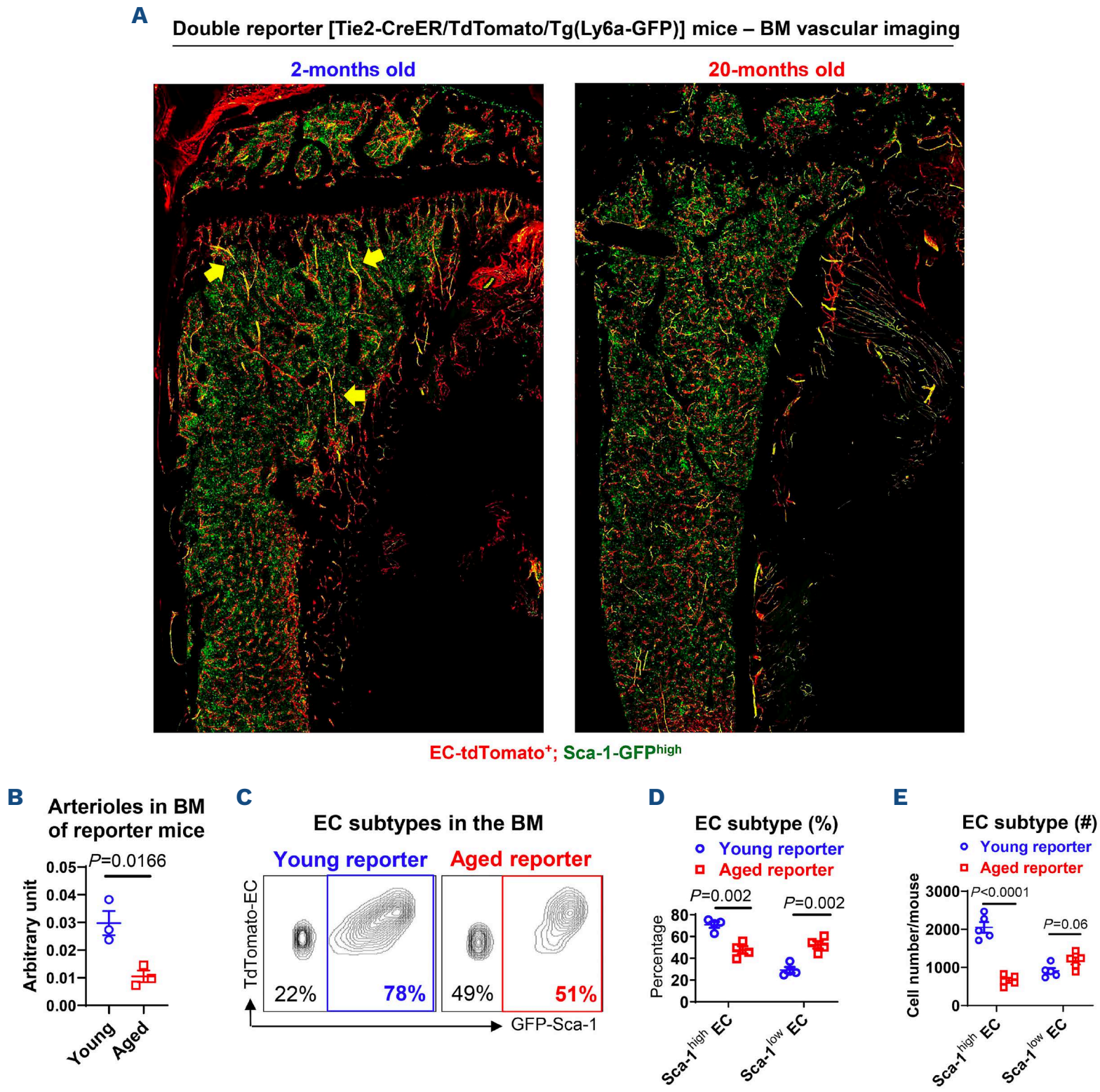

Figure 3. Vascular remodeling of the aged bone marrow niche. (A and B) Representative imaging (A) and quantification (B) of CD31-tdTomato^{+}Sca-1-GFP^{high} endothelial cell (EC)-lined arteriolar vessels (yellow arrows) in tibias from 2 or 20 month old double fluorescent reporter mice (*Tie2-CreER/TdTomato/Tg[Ly6a-GFP]*), following tamoxifen-induced Cre activation, assessed by 3D confocal imaging. (A) One of the three independent experiments with similar results is shown; yellow arrows indicate CD31^{+}Sca-1^{high} EC-lined arteriolar vessels. (C-E) Representative plots (C) and combined results showing frequencies (D) and absolute counts (E) of Sca-1^{high} and Sca-1^{low} EC subfractions in bone marrow (BM) CD45^{-}Ter119^{-}CD31^{+} EC from 2 and 20 month old double reporter mice, analyzed by flow cytometry. Statistical analysis was calculated by two-tailed, unpaired Student *t* test. Results shown represent mean ± standard error of mean.

A

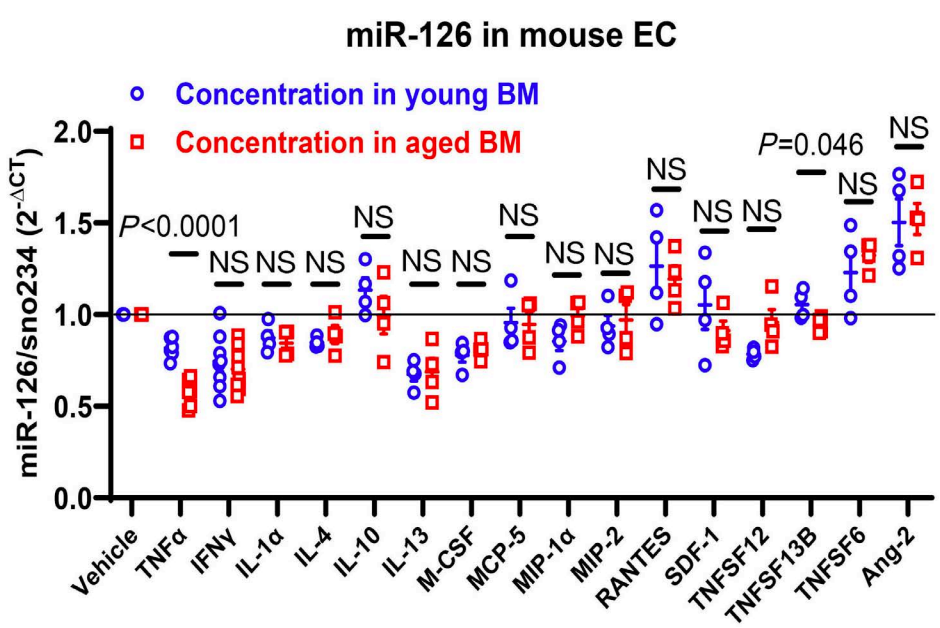

Concentrations (pg/ml)

	Young BM	Aged BM
TNFα	15	22
IFN-γ	64	77
IL-1α	985	1961
IL-4	269	347
IL-10	42	58
IL-13	268	356
IL-16	63508	69456
M-CSF	14	18
MCP-5	88	158
MIP-1α	8.4	37
MIP-2	0.02	2.6
RANTES	1136	3288
SDF-1	14286	16893
TNFSF12	107	225
TNFSF13B	5255	11772
TNFSF6	78	171
Ang-2	4156	5486

B

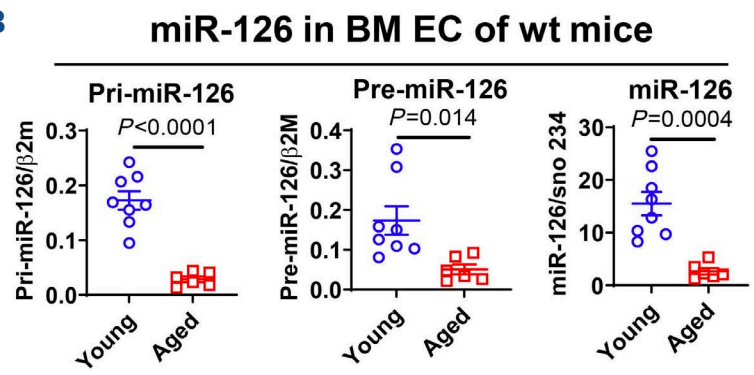

C

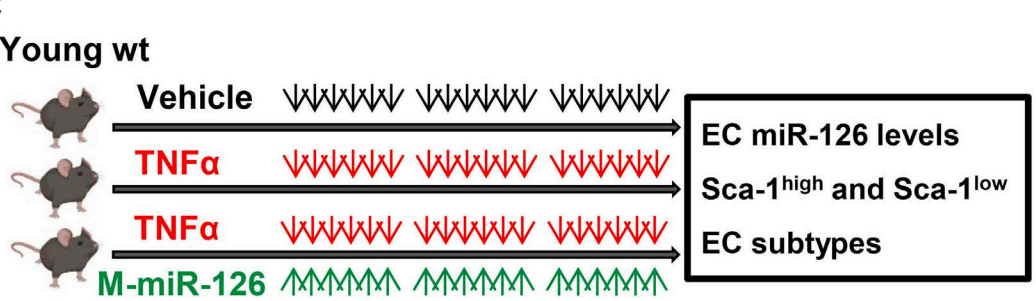

D

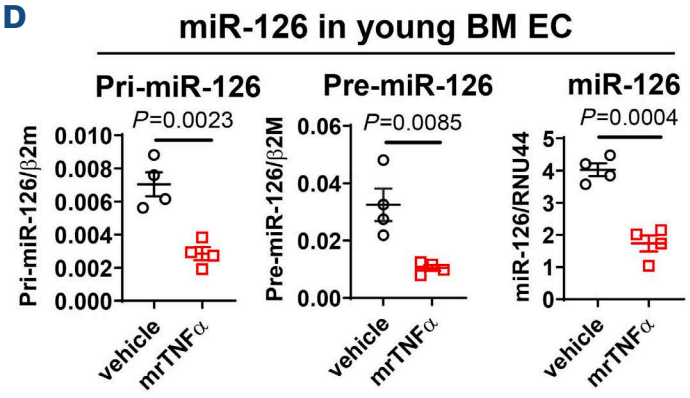

E

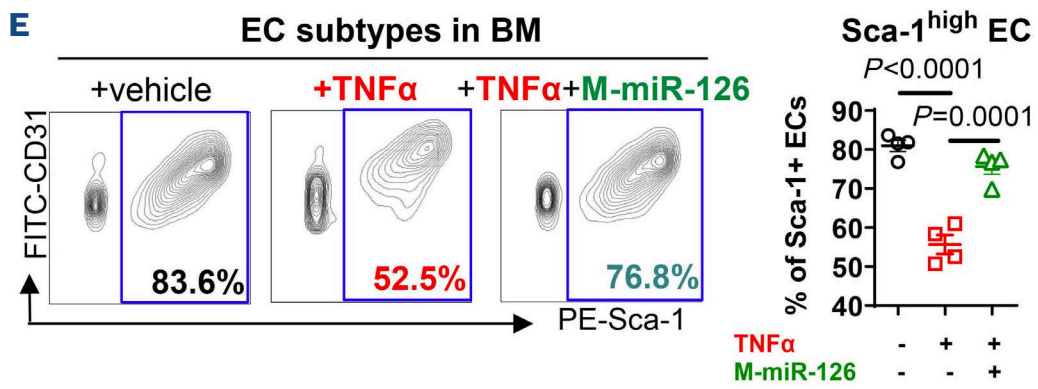

Figure 4. Increased TNFα in aged mice induced endothelial cell miR-126 downregulation. (A) miR-126 levels in mouse endothelial cells (EC) treated with vehicle PBS or individual cytokine for eight hours (left), at the concentrations observed in the bone marrow (BM) of young or aged mice as measured by Luminex assay (right panel), analyzed by quantitative reverse-transcription polymerase chain reaction (Q-RT-PCR) (N=8 for TNFα and TNFSF13B; N=4 for the remaining cytokines). (B) Primary (pri), precursor (pre), and mature miR-126 levels in BM EC from young (2-3-months old, N=8 mice) and aged (18-24-months old, N=6 mice) wild-type (wt) mice, analyzed by Q-RT-PCR. (C-E) Schematic experimental design and results. Young wt mice (2-3-months old, N=4 per group) were treated with vehicle PBS (black arrows), or murine recombinant (mr) TNFα (intraperitoneal [i.p.] 1 µg/day; red arrows) or mrTNFα plus M-miR-126 (intravenous [i.v.] 30 mg/kg; green arrows) for three weeks. (C), BM EC pri, pre, and mature miR-126 levels were measured by Q-RT-PCR (D) and representative plots (E, left) and combined results (E, right) of CD31^{+}Sca-1^{high} and CD31^{+}Sca-1^{low} EC subpopulations were analyzed by flow cytometry. Comparison between groups was performed by two-tailed, unpaired *t* test. Results shown represent mean ± standard error of mean. NS: not significant.

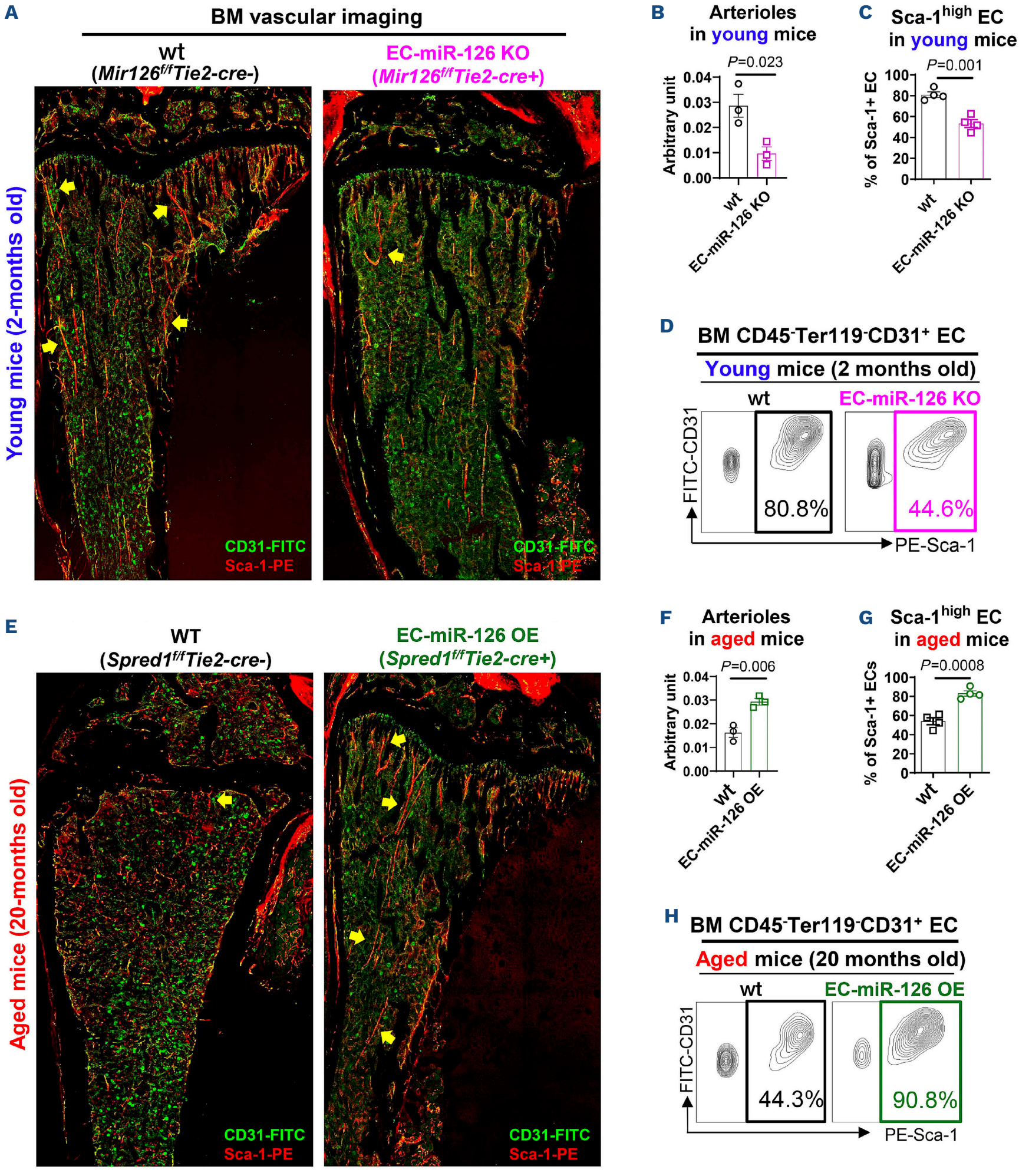

Figure 5. CD31+Sca-1high endothelial cell-lined arterioles reduced in *Mir126f/fTie2-cre+* mice (EC-miR-126 knockout) and increased in *Spred1f/fTie2-cre+* mice (EC-miR-126 overexpression). (A and B) CD31-FITC and Sca-1-PE immunofluorescence staining and 3D confocal imaging (A) and quantification (B) of CD31+Sca-1high endothelial cell (EC)-lined arterioles in tibias from 2-months old *Mir126f/fTie2-cre-* (wild-type [wt]) or *Mir126f/fTie2-cre+* (EC-miR-126 knockout [KO]) mice. (C and D) Combined results (C) and representative plots (D) of Sca-1high and Sca-1low EC subfractions in bone marrow (BM) CD45-Ter119-CD31+ EC from 2-months old *Mir126f/fTie2-cre-* or *Mir126f/fTie2-cre+* mice (N=4 mice per group), analyzed by flow cytometry. (E and F) CD31-FITC and Sca-1-PE immunofluorescence staining and 3D confocal imaging (E) and quantification (F) of CD31+Sca-1high EC-lined arteriolar vessels in tibias

Continued on following page.

from 20-months old *Spred1*$^{f/f}$*Tie2-cre*$^{-}$ (wt) or *Spred1*$^{f/f}$*Tie2-cre*$^{+}$ (EC-miR-126 overexpression [OE]) mice. (G and H) Combined results (G) and representative plots (H) of Sca-1^{high} and Sca-1^{low} EC subfractions in BM CD45^{-}Ter119^{-}CD31^{+} EC from 20-months old *Spred1*$^{f/f}$*Tie2-cre*$^{-}$ or *Spred1*$^{f/f}$*Tie2-cre*$^{+}$ mice (N=4 mice per group), analyzed by flow cytometry. (A and E) One of the three independent experiments with similar results is shown; yellow arrows indicate CD31^{+}Sca-1^{high} EC-lined arteriolar vessels. Comparison between groups was performed by two-tailed, unpaired *t* test. Results shown represent mean ± standard error of mean.

Supplementary Figure S10A, B), and a down-regulator of miR-126 biogenesis.[43,45,46,65] EC-Spred1 KO mice (i.e., *Spred1*$^{f/f}$*Tie2-cre*$^{+}$), therefore, express constitutively higher levels of EC-miR-126 than *Spred1*$^{f/f}$*Tie2-cre*$^{-}$ (wt) control mice (*Online Supplementary Figure S10C*) and represent a functional model for EC-miR-126 OE.[45,46] Accordingly, young *Spred1*$^{f/f}$*Tie2-cre*$^{+}$ mice had more BM arteriole-lining CD31^{+}Sca-1^{high} EC than young wt controls (*Online Supplementary Figure S10D*). Conversely, aged *Spred1*$^{f/f}$*Tie2-cre*$^{+}$ mice did not display loss of CD31^{+}Sca-1^{high} EC-lined arteriolar vessels such as those seen in aged wt controls (Figure 5E-H).

Taken together, these results support a model in which "inflammaging" suppresses endothelial miR-126 expression, resulting in loss of CD31^{+}Sca-1^{high} EC and reduced arteriolar density in the aged BM niche.

miR-126 downregulation in aged bone marrow endothelial cells contributes to loss of regenerating capacity of hematopoietic stem cells

MiR-126 regulates the self-renewal capacity of HSC.[41-43] In the BM niche of normal wt mice, we found that EC expressed at least a log-fold higher level of miR-126 than HSC (Fit3^{-}CD150^{+}CD48^{-} LSK).[43,45,46] While HSC may produce endogenous miR-126, miR-126^{high} EC lining BM arteriolar vessels also supply miR-126 to surroundings cells in the BM niche, including HSC.[43,45,46] We previously demonstrated that BM EC deliver mature miR-126 to leukemia stem cells (LSC) and HSC through extracellular vesicles.[43] Thus, a decline in BM CD31^{+}Sca-1^{high} EC-lined arterioles as observed in the aged BM niche, could reduce the exogenous supply of EC-derived miR-126 to HSC, ultimately impairing hematopoietic activity by promoting HSC expansion at the expense of their self-renewal capacity. Accordingly, while levels of pri- and pre-miR-126 were similar in young and aged BM HSC, mature miR-126 levels were significantly reduced in HSC from the aged mice (Figure 6A), which also displayed a reduction of miR-126^{high} CD31^{+}Sca-1^{high} arterioles (Figure 2A, B) and lower HSC self-renewal capacity (Figure 1A, B and *Online Supplementary Figure S1A, B*). We observed that these features were remarkably similar to those observed in young EC-miR-126 KO mice (*Mir126*$^{f/f}$*Tie2-cre*$^{+}$) that, like aged wt mice, had low miR-126 levels (*Online Supplementary Figure S8A*), reduction of CD31^{+}Sca-1^{high} arterioles (Figure 5A-D), and expansion of BM HSC (Figure 6B), yet, despite their young age, showed a significantly impaired long-term regenerating capacity compared with young wt mice (*Mir126*$^{f/f}$*Tie2-cre*$^{+}$ HSC *vs*. *Mir126*$^{f/f}$*Tie2-cre*$^{-}$ HSC engraftment rates: 41% *vs*. 62% at 20 weeks post transplant, *P*=0.0385) (Figure 6C, D). Conversely, aged EC-miR-126 OE mice (*Spred1*$^{f/f}$*Tie2-cre*$^{+}$) had higher density of BM CD31^{+}Sca-1^{high} EC and arterioles (Figure 5E-H) and lower frequency of HSC (Figure 7A), which exhibited enhanced self-renewal capacity compared with aged wt controls (*Spred1*$^{f/f}$*Tie2-cre*$^{+}$ HSC *vs*. *Spred1*$^{f/f}$*Tie2-cre*$^{-}$ HSC engraftment rates: 42% *vs*. 9% at 20 weeks post transplant, *P*=0.0016) (Figure 7B, C). Finally, aged HSC from CD45.2 mice (20 months old) co-cultured with aged EC had lower levels of miR-126 and reduced long-term engraftment rates in congenic CD45.1 recipients compared with aged HSC co-cultured with young EC (engraftment at 16 weeks post transplant: 46.2% *vs*. 65.7%, *P*=0.0003) (Figure 7D); this reduction could be rescued by co-treatment with miR-126 mimic (engraftment at 16 weeks: 46.2% *vs*. 57.2%, *P*=0.03) (Figure 7D).

These findings further support the hypothesis that EC miR-126 reduction, whether due to aging or genetic deletion, drives HSC expansion at the cost of long-term self-renewal capacity.

Reduced metabolism in aged hematopoietic stem cells

To gain insight into the intrinsic molecular mechanism underlying the reduced self-renewal capacity in aged HSC upon decreased EC miR-126 supply, we performed RNA-seq of BM HSC from young (N=3 samples, pooled from 30 young mice) and aged (N=3 samples, from 3 aged mice) mice. We identified 388 up-regulated and 127 down-regulated genes in aged *versus* young HSC. GSEA revealed upregulation of inflammation-response gene sets (e.g., interferon alpha response, IL2-STAT5 signaling, interferon gamma response, IL6-JAK-STAT3 signaling, inflammatory response) and down-regulation of gene sets related to DNA repair, mitotic spindle, G2M checkpoint, and E2F targets in aged HSC compared with young HSC (*Online Supplementary Figures S11A, B and S12A, B*). Aged HSC seemingly acquired a lineage-biased profile with higher levels of myeloid (i.e., Cebpd, Itgam, Csf3r, Hk3, Elane, Csf2ra)[66,67] and megakaryocyte (i.e., Mpl, Vwf, Slamf1)[68] associated marker genes (*Online Supplementary Figure S13A, B*). Aged HSC also have higher expression levels of miR-126 target genes (i.e., Adam9, Cdk3, Itga6, Cd84, Hoxb6 and PLK2),[41,69,70] consistent with their lower miR-126 levels than young HSC (*Online Supplementary Figure S13B*). Notably, aged HSC exhibited a significant downregulation of gene sets involved in oxidative phosphorylation (OXPHOS) (*Online Supplementary Figures S11B, S14A, B,* and *S15A, B*). In line with this transcriptional profile, aged HSC demonstrated reduced OXPHOS (measured by oxygen consumption rate [OCR]) and glycolysis (measured by extracellular

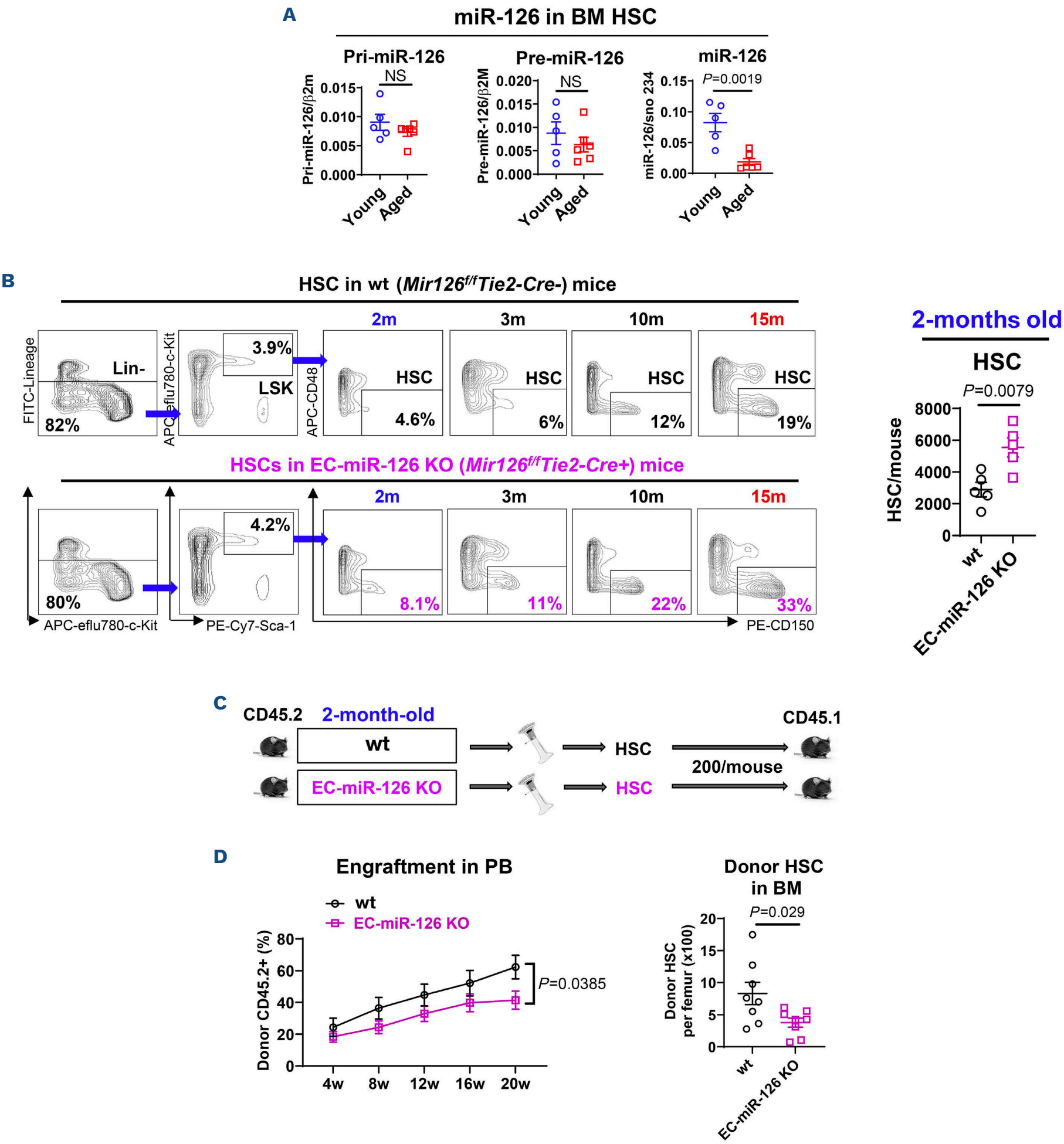

Figure 6. miR-126 downregulation in bone marrow endothelial cells contributes to loss of regenerating capacity of hematopoietic stem cells. (A) Primary (Pri-), precursor (pre-), and mature miR-126 levels in bone marrow (BM) lineage-Sca-1$^+$c-Kit$^+$FLT3$^-$CD150$^+$CD48$^-$ hematopoietic stem cells (HSC) from young (2-3-months old) and aged (18-24-months old) mice by quantitative reverse-transcription polymerase chain reaction (Q-RT-PCR). (B) Representative plots (left) and combined results (right, N=5 mice per group) of BM lineage$^-$Sca-1$^+$c-Kit$^+$FLT3$^-$CD150$^+$CD48$^-$ HSC in 2-, 3-, 10-, and 15-months (m) old *Mir126*$^{f/f}$*Tie2-cre*$^-$ (wild-type [wt]) and *Mir126*$^{f/f}$*Tie2-cre*$^+$ (endothelial cell [EC]-miR-126 knockout [KO]) mice. (C and D) Lineage$^-$Sca-1$^+$c-Kit$^+$FLT3$^-$CD150$^+$CD48$^-$ HSC from 2-months old *Mir126*$^{f/f}$*Tie2-cre*$^-$ (wt) or *Mir126*$^{f/f}$*Tie2-cre*$^+$ (EC-miR-126 KO) mice (CD45.2) were transplanted into 2-months old CD45.1 recipient mice (C) and donor HSC engraftment rates (% of CD45.2$^+$) in peripheral blood (PB) monthly and donor lineage-Sca-1$^+$c-Kit$^+$FLT3$^-$CD150$^+$CD48$^-$ HSC number in BM of the recipient mice at 20 weeks post transplant were analyzed by flow cytometry (D). Comparison between groups was performed by two-tailed, unpaired *t* test. Results shown represent mean ± standard error of mean. NS: not significant.

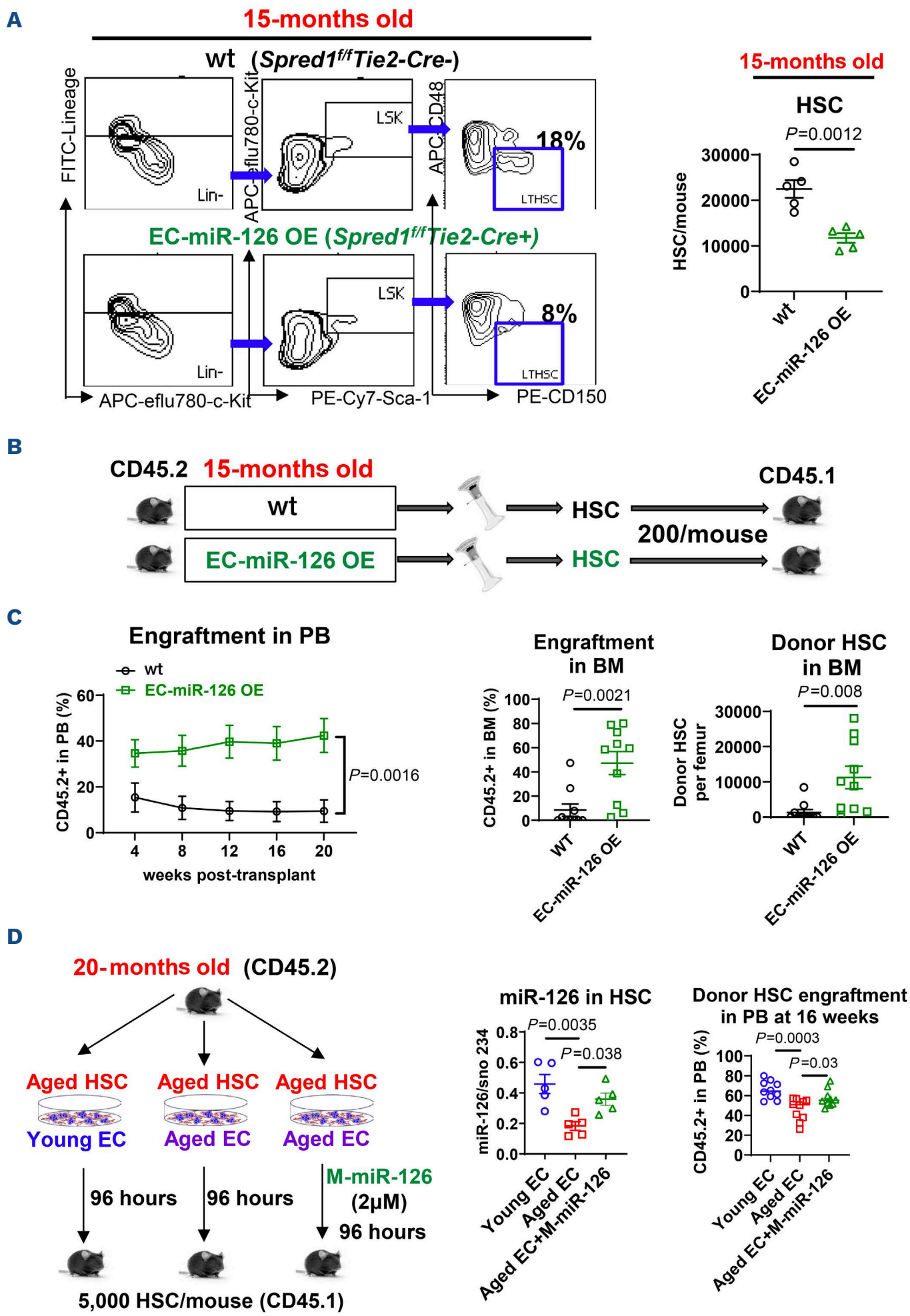

Figure 7. Upregulation of endothelial cell-miR-126 contributes to increased long-term regenerating capacity in aged hematopoietic stem cells. (A) Representative plots (left) and combined results (right, N=5 mice per group) of bone marrow (BM) lineage$^-$Sca-1$^+$c-Kit$^+$FLT3$^-$CD150$^+$CD48$^-$ hematopoietic stem cells (HSC) in 15-months (m) old *Spred1*$^{f/f}$*Tie2-cre*$^-$ (wild-type [wt]) and *Spred1*$^{f/f}$*Tie2-cre*$^+$ (endothelial cell [EC]-miR-126 overexpression [OE]) mice. (B and C) Lineage$^-$Sca-1$^+$c-Kit$^+$FLT3$^-$CD150$^+$CD48$^-$ HSC from 15-months old *Spred1*$^{f/f}$*Tie2-cre*$^-$ (wt) or *Spred1*$^{f/f}$*Tie2-cre*$^+$ (EC-miR-126 OE) mice (CD45.2) were transplanted into 2-months old CD45.1 recipient mice (B) and donor HSC engraftment rates in peripheral blood (PB) of the recipient mice monthly and in BM at 20 weeks post transplant were analyzed by flow cytometry (C). (D) Lineage$^-$Sca-1$^+$c-Kit$^+$FLT3$^-$CD150$^+$CD48$^-$ HSC from aged mice (CD45.2, 20-months old) were co-cultured with young or aged EC, respectively, collected from 2-3 months old or 18-24 months old mice, for 96 hours. HSC co-cultured with aged EC were also treated with miR-126 mimic (M-miR-126, 2 μM; 96 hours). HSC were collected and miR-126 levels were analyzed by quantitative reverse-transcription polymerase chain reaction

(Q-RT-PCR). HSC were also transplanted into CD45.1 recipient mice and engraftment rates were monitored monthly by flow cytometry analysis. SCR: scrambled RNA control. Comparison between groups was performed by two-tailed, unpaired *t* test. Results shown represent mean ± standard error of mean.

acidification rate [ECAR]) activity and ATP production using the Seahorse assay, and impaired mitochondrial fusion,[71] as assessed by electron microscopy (*Online Supplementary Figure S16A-D*). To confirm that these metabolic changes occurring in aged HSC were driven by reduced miR-126 expression, we treated aged HSC with miR-126 mimic (2 μM). Compared to scramble controls, miR-126 mimic partly rescued the changes associated with miR-126 depletion, as it increased OXPHOS, glycolysis and ATP, and restored mitochondrial fusion (*Online Supplementary Figure S17A-D*).

Discussion

There is growing evidence to indicate that aged mice present with BM vascular niche remodeling and loss of HSC self-renewal capacity with skewed myeloid / megakaryocytic differentiation compared with young mice.[26,72] Whether the age-related inflammation of the BM niche is the primary cause or a direct consequence of HSC aging is not fully understood. With age, arteriolar vessels decrease, while sinusoids appear largely unchanged.[72] The vessel changes result in increase in the vascular leakiness and reactive oxygen species levels and decrease in angiogenesis.[32] Poulos *et al*. previously reported that young HSC co-cultured with aged EC lack long-term hematopoietic multilineage reconstitution, while aged HSC co-cultured with young EC maintain their self-renewal ability.[32] Infusion of young EC into aged, conditioned mice rejuvenates an aged hematopoietic system.[32] Thus, a disrupted interplay between the vascular component of the BM niche and HSC may play a significant role in those functional changes observed in aged hematopoiesis; however, the molecular mechanisms remain to be fully elucidated.

MiR-126 is one of the most highly expressed microRNA in EC, where it acts as a master regulator of angiogenesis.[38,40] miR-126 reportedly regulates many aspects of EC biology and contributes to the maintenance of vascular integrity and inhibition of endothelial permeability by inhibiting its targets, SPRED1 and PIK3R2, the negative regulators of the VEGF pathway,[38,40] and other vascular secretory factors, including VEGF itself.[73] We previously showed that BM CD31^{+}Sca-1^{high} EC (that line mainly arterioles) express the highest levels of miR-126 in the BM niche and supply miR-126 to HSC to maintain their homeostasis, quiescence and self-renewal capacity.[43]

Here, we used young and aged wt and EC/Sca-1 reporter mice, an EC-miR-126 KO model, and a functional model for EC-miR-126 OE (EC-Spred1 KO) to study the vascular changes occurring in the aged BM niche and their impact on HSC aging. Several additional biomarkers (e.g., phosphorylation status of α-SMA, VE-cadherin) were used by other groups to identify specific vessels;[74,75] however, due to technical challenges in imaging bone with confocal microscopy, and the lack of a "gold standard" immunostaining classification of BM vessels, based on our publications and other reports,[27,31,43,45] we here chose to combine CD31/Sca-1 immunofluorescent staining, 3D confocal imaging and flow cytometry analysis of long bone and marrow cells to identify and quantify vascular changes in the aged BM niche. We showed that aged mice had lower levels of EC-miR-126 and undergo a BM vascular remodeling, with a loss in CD31^{+}Sca-1^{high} EC, which line mainly non-permeable arterioles, and a gain in CD31^{+}Sca-1^{low} EC, which line mainly fenestrated, permeable sinusoids. These alterations were phenocopied in EC-miR-126 KO mice and rescued in EC-miR-126 OE (i.e., EC-Spred1 KO) mice. Of note, while EC-Spred1 KO is a validated method to elevate EC-miR-126 levels,[43,45,46,65] it cannot fully exclude its contribution independently of miR-126 levels to vascular changes. Nevertheless, when considered altogether, our data collectively support a causal link between miR-126 downregulation and arteriole loss in aged BM. To this end, we and others have identified miR-126 as a key regulator of angiogenic signaling and vascular integrity.[38,40,45] Here, we extend these findings to the aging BM niche, demonstrating that EC-specific miR-126 loss drives arteriole depletion, thereby limiting the arteriolar supply of miR-126 to HSC. The role of miR-126 in regulating HSC homeostasis and self-renewal capacity has been well characterized.[41-43] Here, we specifically examine how aging perturbs the EC–HSC crosstalk in the BM niche, thereby resulting in hematopoietic dysfunction. Our results indicate that aging-related hematopoietic dysfunction and vascular remodeling likely occur in parallel and could reinforce one another through the disrupted miR-126 trafficking from EC to HSC. Of note, the BM vascular niche provides HSC-supportive cues (including oxygen, nutrients, and signaling molecules[76]) that likely act in synergy with miR-126-dependent pathways, and how these factors change during aging, in addition to miR-126, should be dissected in future studies.

In aged mice, the BM microenvironment is reportedly associated with increased pro-inflammatory cytokines, and skewing of HSC to myeloid differentiation.[16] We showed that in the aged BM niche, levels of inflammatory cytokines are elevated, and while HSC expand, they have a significantly reduced regenerative capacity, in addition to myeloid / megakaryocytic skewing. Mature myeloid / megakaryocytic cells are a major source of inflammatory cytokines[77] that further amplify myeloid/megakaryocytic differentiation[72,78-80] and increase BM "inflammaging". While several inflammatory

cytokines have been reported to mediate the "inflammaging",[15] we have focused on TNFα which has been intensively studied for its role in both normal and malignant hematopoiesis.[80,81] Yamashita and Passegue recently reported that TNFα might lead to hyperproliferation of HSC and exacerbated myelopoiesis in aging.[80] Here, we show that TNFα-induced downregulation of EC-miR-126 results in depletion of miR-126^{high} CD31^{+}Sca-1^{high} EC and gain in miR-126^{low} CD31^{+}Sca-1^{low} EC, causing loss of arterioles and enrichment of sinusoids. This age-related BM vascular remodeling reduces the supply of EC miR-126 to HSC, which expand but lose long-term regenerating capacity. Of note, the decrease in CD31^{+}Sca-1^{high} EC and arterioles and expansion of HSC with reduced regenerating capacity in the aged BM niche were recapitulated in the young EC-miR-126 KO mice. To this end, up-regulating miR-126 levels by synthetic miR-126 mimic rescued the reduction of long-term hematopoietic regenerating capacity in aged HSC co-cultured with aged EC compared with those co-cultured with young EC.

In conclusion, our findings establish miR-126 as a critical regulator of BM vascular integrity and HSC maintenance during aging. In our model, aged HSC expand and generate myeloid cells that secrete inflammatory cytokines including TNFα. Elevated TNFα in the aging BM niche suppresses EC-miR-126, disrupts arteriolar architecture, and diminishes miR-126 availability to HSC, contributing to their functional decline. Therapeutic restoration of miR-126 using synthetic mimic may represent a promising strategy to counteract aging-associated hematopoietic dysfunction and rejuvenate hematopoiesis.

Disclosures

GM holds patent positions, stock and royalty interests in Ostentus Therapeutics, none of which interests funded, contributed to or influenced the work described here. All the other authors have no conflicts of interest to disclose.

Contributions

DZ, LN, XG, FC and XZ conducted experiments and analyzed data; MC analyzed RNA-seq data; GM reviewed the manuscript and provided administrative support; BZ designed experiments, analyzed data, wrote the manuscript, and provided administrative support. All authors approved the final version of the manuscript for publication.

Acknowledgments

We acknowledge the support of the Animal Resources Center, Analytical Cytometry, Integrative Genomics, and DNA/RNA Shared Resources at City of Hope Comprehensive Cancer Center supported by the National Cancer Institute of the National Institutes of Health under grant number P30CA033572.

Funding

This work was supported in part by National Cancer Institute grants CA248475 (to GM and BZ), CA258981(to GM and BZ), CA286160 (to BZ and GM), and P30CA033572, and by the Robert and Lynda Altman Family Foundation Research Fund.

Data-sharing statement

The RNA-seq data (GSE296123) generated in this study are available at the Gene Expression Omnibus (GEO) repository of the National Center for Biotechnology Information (https://www.ncbi.nlm.nih.gov/geo/query/acc.cgi?&acc=GSE296123; reviewer token: gxijyayutjatzux). Additional information, including the Online Supplementary Methods and Online Supplementary Figures, are provided in the online version of this paper. All other datasets generated during this study are available from the corresponding author on reasonable request.

References

1. Dykstra B, Kent D, Bowie M, et al. Long-term propagation of distinct hematopoietic differentiation programs in vivo. Cell Stem Cell. 2007;1(2):218-229.
2. Wilkinson AC, Igarashi KJ, Nakauchi H. Haematopoietic stem cell self-renewal in vivo and ex vivo. Nat Rev Genet. 2020;21(9):541-554.
3. Haas S, Trumpp A, Milsom MD. Causes and consequences of hematopoietic stem cell heterogeneity. Cell Stem Cell. 2018;22(5):627-638.
4. Morita Y, Ema H, Nakauchi H. Heterogeneity and hierarchy within the most primitive hematopoietic stem cell compartment. J Exp Med. 2010;207(6):1173-1182.
5. Sanjuan-Pla A, Macaulay IC, Jensen CT, et al. Platelet-biased stem cells reside at the apex of the haematopoietic stem-cell hierarchy. Nature. 2013;502(7470):232-236.
6. Su TY, Hauenstein J, Somuncular E, et al. Aging is associated with functional and molecular changes in distinct hematopoietic stem cell subsets. Nat Commun. 2024;15(1):7966.
7. de Haan G, Lazare SS. Aging of hematopoietic stem cells. Blood. 2018;131(5):479-487.
8. Rossi DJ, Jamieson CH, Weissman IL. Stems cells and the pathways to aging and cancer. Cell. 2008;132(4):681-696.
9. Zhang L, Mack R, Breslin P, Zhang J. Molecular and cellular mechanisms of aging in hematopoietic stem cells and their niches. J Hematol Oncol. 2020;13(1):157.
10. Mejia-Ramirez E, Florian MC. Understanding intrinsic hematopoietic stem cell aging. Haematologica. 2020;105(1):22-37.
11. Zhao Y, Simon M, Seluanov A, Gorbunova V. DNA damage and repair in age-related inflammation. Nat Rev Immunol. 2023;23(2):75-89.
12. Stead ER, Bjedov I. Balancing DNA repair to prevent ageing and cancer. Exp Cell Res. 2021;405(2):112679.
13. Amorim JA, Coppotelli G, Rolo AP, Palmeira CM, Ross JM, Sinclair DA. Mitochondrial and metabolic dysfunction in ageing and age-related diseases. Nat Rev Endocrinol. 2022;18(4):243-258.
14. Miwa S, Kashyap S, Chini E, von Zglinicki T. Mitochondrial

dysfunction in cell senescence and aging. J Clin Invest. 2022;132(13):e158447.
15. Li X, Li C, Zhang W, Wang Y, Qian P, Huang H. Inflammation and aging: signaling pathways and intervention therapies. Signal Transduct Target Ther. 2023;8(1):239.
16. Franceschi C, Garagnani P, Parini P, Giuliani C, Santoro A. Inflammaging: a new immune-metabolic viewpoint for age-related diseases. Nat Rev Endocrinol. 2018;14(10):576-590.
17. Herr LM, Schaffer ED, Fuchs KF, Datta A, Brosh RM Jr. Replication stress as a driver of cellular senescence and aging. Commun Biol. 2024;7(1):616.
18. Burhans WC, Weinberger M. DNA replication stress, genome instability and aging. Nucleic Acids Res. 2007;35(22):7545-7556.
19. D'Amico AM, Vasquez KM. The multifaceted roles of DNA repair and replication proteins in aging and obesity. DNA Repair (Amst). 2021;99:103049.
20. Clarke TL, Mostoslavsky R. DNA repair as a shared hallmark in cancer and ageing. Mol Oncol. 2022;16(18):3352-3379.
21. Saleh Z, Mirzazadeh S, Mirzaei F, Heidarnejad K, Meri S, Kalantar K. Alterations in metabolic pathways: a bridge between aging and weaker innate immune response. Front Aging. 2024;5:1358330.
22. Khalaf F, Barayan D, Saldanha S, Jeschke MG. Metabolaging: a new geroscience perspective linking aging pathologies and metabolic dysfunction. Metabolism. 2025;166:156158.
23. Farahzadi R, Valipour B, Montazersaheb S, Fathi E. Targeting the stem cell niche micro-environment as therapeutic strategies in aging. Front Cell Dev Biol. 2023;11:1162136.
24. Matteini F, Mulaw MA, Florian MC. Aging of the hematopoietic stem cell niche: new tools to answer an old question. Front Immunol. 2021;12:738204.
25. Gao X, Zhang J, Tamplin OJ. The aging hematopoietic stem cell niche: a mini review. Front Hematol. 2025;4:1525132.
26. Ho YH, Mendez-Ferrer S. Microenvironmental contributions to hematopoietic stem cell aging. Haematologica. 2020;105(1):38-46.
27. Itkin T, Gur-Cohen S, Spencer JA, et al. Distinct bone marrow blood vessels differentially regulate haematopoiesis. Nature. 2016;532(7599):323-328.
28. Liu X, Zhang P, Gu Y, Guo Q, Liu Y. Type H vessels: functions in bone development and diseases. Front Cell Dev Biol. 2023;11:1236545.
29. Peng Y, Wu S, Li Y, Crane JL. Type H blood vessels in bone modeling and remodeling. Theranostics. 2020;10(1):426-436.
30. Sivaraj KK, Adams RH. Blood vessel formation and function in bone. Development. 2016;143(15):2706-2715.
31. Kunisaki Y, Bruns I, Scheiermann C, et al. Arteriolar niches maintain haematopoietic stem cell quiescence. Nature. 2013;502(7473):637-643.
32. Poulos MG, Ramalingam P, Gutkin MC, et al. Endothelial transplantation rejuvenates aged hematopoietic stem cell function. J Clin Invest. 2017;127(11):4163-4178.
33. Turko R, Hajja A, Magableh AM, et al. The emerging role of miRNAs in biological aging and age-related diseases. Noncoding RNA Res. 2025;13:131-152.
34. ElSharawy A, Keller A, Flachsbart F, et al. Genome-wide miRNA signatures of human longevity. Aging Cell. 2012;11(4):607-616.
35. de Almeida-Faria J, Duque-Guimaraes DE, Ong TP, et al. Maternal obesity during pregnancy leads to adipose tissue ER stress in mice via miR-126-mediated reduction in Lunapark. Diabetologia. 2021;64(4):890-902.
36. Tomasetti M, Nocchi L, Staffolani S, et al. MicroRNA-126 suppresses mesothelioma malignancy by targeting IRS1 and interfering with the mitochondrial function. Antioxid Redox Signal. 2014;21(15):2109-2125.
37. Zhao YY, Nogueira MS, Milne GL, et al. Association between lipid peroxidation biomarkers and microRNA expression profiles. Redox Biol. 2022;58:102531.
38. Fish JE, Santoro MM, Morton SU, et al. miR-126 regulates angiogenic signaling and vascular integrity. Dev Cell. 2008;15(2):272-284.
39. Kuhnert F, Mancuso MR, Hampton J, et al. Attribution of vascular phenotypes of the murine Egfl7 locus to the microRNA miR-126. Development. 2008;135(24):3989-3993.
40. Wang S, Aurora AB, Johnson BA, et al. The endothelial-specific microRNA miR-126 governs vascular integrity and angiogenesis. Dev Cell. 2008;15(2):261-271.
41. Lechman ER, Gentner B, Ng SWK, et al. miR-126 regulates distinct self-renewal outcomes in normal and malignant hematopoietic stem cells. Cancer Cell. 2016;29(4):602-606.
42. Lechman ER, Gentner B, van Galen P, et al. Attenuation of miR-126 activity expands HSC in vivo without exhaustion. Cell Stem Cell. 2012;11(6):799-811.
43. Zhang B, Nguyen LXT, Li L, et al. Bone marrow niche trafficking of miR-126 controls the self-renewal of leukemia stem cells in chronic myelogenous leukemia. Nat Med. 2018;24(4):450-462.
44. Sessa R, Seano G, di Blasio L, et al. The miR-126 regulates angiopoietin-1 signaling and vessel maturation by targeting p85beta. Biochim Biophys Acta. 2012;1823(10):1925-1935.
45. Zhang B, Nguyen LXT, Zhao D, et al. Treatment-induced arteriolar revascularization and miR-126 enhancement in bone marrow niche protect leukemic stem cells in AML. J Hematol Oncol. 2021;14(1):122.
46. Qiao J, Zhao D, Nguyen LXT, et al. Targeting miR-126 in Ph+ acute lymphoblastic leukemia. Leukemia. 2023;37(7):1540-1544.
47. Kusumbe AP, Ramasamy SK, Starsichova A, Adams RH. Sample preparation for high-resolution 3D confocal imaging of mouse skeletal tissue. Nat Protoc. 2015;10(12):1904-1914.
48. Passaro D, Di Tullio A, Abarrategi A, et al. Increased vascular permeability in the bone marrow microenvironment contributes to disease progression and drug response in acute myeloid leukemia. Cancer Cell. 2017;32(3):324-341.e326.
49. Anders S, Huber W. Differential expression analysis for sequence count data. Genome Biol. 2010;11(10):R106.
50. McCarthy DJ, Chen Y, Smyth GK. Differential expression analysis of multifactor RNA-Seq experiments with respect to biological variation. Nucleic Acids Res. 2012;40(10):4288-4297.
51. Robinson MD, McCarthy DJ, Smyth GK. edgeR: a Bioconductor package for differential expression analysis of digital gene expression data. Bioinformatics. 2010;26(1):139-140.
52. Wu T, Hu E, Xu S, et al. clusterProfiler 4.0: a universal enrichment tool for interpreting omics data. Innovation (Camb). 2021;2(3):100141.
53. Xu S, Hu E, Cai Y, et al. Using clusterProfiler to characterize multiomics data. Nat Protoc. 2024;19(11):3292-3320.
54. Yu G. Thirteen years of clusterProfiler. Innovation (Camb). 2024;5(6):100722.
55. Yu GC, Wang LG, Han YY, He QY. clusterProfiler: an R package for comparing biological themes among gene clusters. OMICS. 2012;16(5):284-287.
56. Wang L, Zhou F, Zhang P, et al. Human type H vessels are a sensitive biomarker of bone mass. Cell Death Dis. 2017;8(5):e2760.
57. Ramasamy SK. Structure and functions of blood vessels and vascular niches in bone. Stem Cells Int. 2017;2017:5046953.
58. Ferrucci L, Fabbri E. Inflammageing: chronic inflammation in ageing, cardiovascular disease, and frailty. Nat Rev Cardiol.

2018;15(9):505-522.
59. Bogeska R, Mikecin AM, Kaschutnig P, et al. Inflammatory exposure drives long-lived impairment of hematopoietic stem cell self-renewal activity and accelerated aging. Cell Stem Cell. 2022;29(8):1273-1284.e1278.
60. Bousounis P, Bergo V, Trompouki E. Inflammation, aging and hematopoiesis: a complex relationship. Cells. 2021;10(6):1386.
61. Kovtonyuk LV, Fritsch K, Feng XM, Manz MG, Takizawa H. Inflamm-aging of hematopoiesis, hematopoietic stem cells, and the bone marrow microenvironment. Front Immunol. 2016;7:502.
62. Mahamud MR, Geng X, Ho YC, et al. GATA2 controls lymphatic endothelial cell junctional integrity and lymphovenous valve morphogenesis through miR-126. Development. 2019;146(21):dev184218.
63. Harris TA, Yamakuchi M, Kondo M, Oettgen P, Lowenstein CJ. Ets-1 and Ets-2 regulate the expression of microRNA-126 in endothelial cells. Arterioscler Thromb Vasc Biol. 2010;30(10):1990-1997.
64. Hartmann D, Fiedler J, Sonnenschein K, et al. MicroRNA-based therapy of GATA2-deficient vascular disease. Circulation. 2016;134(24):1973-1990.
65. Qiao J, Liang C, Zhao D, et al. Spred1 deficit promotes treatment resistance and transformation of chronic phase CML. Leukemia. 2022;36(2):492-506.
66. Chen F, Zhao D, Xu Y, et al. miR-142 deficit in T cells during blast crisis promotes chronic myeloid leukemia immune escape. Nat Commun. 2025;16(1):1253.
67. Zhang B, Zhao D, Chen F, et al. Acquired miR-142 deficit in leukemic stem cells suffices to drive chronic myeloid leukemia into blast crisis. Nat Commun. 2023;14(1):5325.
68. Carrelha J, Meng Y, Kettyle LM, et al. Hierarchically related lineage-restricted fates of multipotent haematopoietic stem cells. Nature. 2018;554(7690):106-111.
69. Guo B, Gu J, Zhuang T, et al. MicroRNA-126: from biology to therapeutics. Biomed Pharmacother. 2025;185:117953.
70. Yan Y, Wang R, Hu X, et al. MiR-126 regulates properties of SOX9(+) liver progenitor cells during liver repair by targeting Hoxb6. Stem Cell Rep. 2020;15(3):706-720.
71. Chen W, Zhao H, Li Y. Mitochondrial dynamics in health and disease: mechanisms and potential targets. Signal Transduct Target Ther. 2023;8(1):333.
72. Ho YH, Del Toro R, Rivera-Torres J, et al. Remodeling of bone marrow hematopoietic stem cell niches promotes myeloid cell expansion during premature or physiological aging. Cell Stem Cell. 2019;25(3):407-418.e406.
73. Liu B, Peng XC, Zheng XL, Wang J, Qin YW. MiR-126 restoration down-regulate VEGF and inhibit the growth of lung cancer cell lines in vitro and in vivo. Lung Cancer. 2009;66(2):169-175.
74. Chen L, DeWispelaere A, Dastvan F, et al. Smooth muscle-alpha actin inhibits vascular smooth muscle cell proliferation and migration by inhibiting Rac1 activity. PLoS One. 2016;11(5):e0155726.
75. Vestweber D. VE-cadherin: the major endothelial adhesion molecule controlling cellular junctions and blood vessel formation. Arterioscler Thromb Vasc Biol. 2008;28(2):223-232.
76. Chen J, Hendriks M, Chatzis A, Ramasamy SK, Kusumbe AP. Bone vasculature and bone marrow vascular niches in health and disease. J Bone Miner Res. 2020;35(11):2103-2120.
77. Pietras EM. Inflammation: a key regulator of hematopoietic stem cell fate in health and disease. Blood. 2017;130(15):1693-1698.
78. Haas S, Hansson J, Klimmeck D, et al. Inflammation-induced emergency megakaryopoiesis driven by hematopoietic stem cell-like megakaryocyte progenitors. Cell Stem Cell. 2015;17(4):422-434.
79. Pietras EM, Mirantes-Barbeito C, Fong S, et al. Chronic interleukin-1 exposure drives haematopoietic stem cells towards precocious myeloid differentiation at the expense of self-renewal. Nat Cell Biol. 2016;18(6):607-618.
80. Yamashita M, Passegue E. TNF-alpha coordinates hematopoietic stem cell survival and myeloid regeneration. Cell Stem Cell. 2019;25(3):357-372.e357.
81. Silke J, Hartland EL. Masters, marionettes and modulators: intersection of pathogen virulence factors and mammalian death receptor signaling. Curr Opin Immunol. 2013;25(4):436-440.